Hierarchical Surface Topography in Block Copolymer Thin Films Induced by Residual Solvent

Seung-Heon Lee,† Huiman Kang, Youn Sang Kim, and Kookheon Char*

School of Chemical Engineering and Institute of Chemical Processes, Seoul National University, Seoul 151-744, Korea

Received November 1, 2002; Revised Manuscript Received April 3, 2003

ABSTRACT: We have investigated the hierarchical surface topography in block copolymer thin films induced by residual solvent using optical microscopy and atomic force microscopy. A polystyrene−poly(2-vinylpyridine) (PS−P2VP) block copolymer forming lamellar morphology was spun-cast from *N*,*N*-dimethylformamide (DMF) solution onto a silicon wafer with a native oxide layer. Thin films with various thicknesses between $2.0L_0$ and $3.5L_0$, where L_0 is the equilibrium lamellar period, were prepared. Typical multilayered lamellae having either islands or holes with quantized thicknesses were observed after annealing at 180 °C due to the strong affinity of the P2VP blocks toward the Si substrate and the preferential wetting of the PS blocks at the free surface. Further annealing, however, resulted in the formation of hierarchical surface topography such as *hole-in-hole* and/or *island-on-island* morphology. In addition, holes adjacent to the brush layer with $L_0/2$ thickness tightly bound to the substrate were found to be fractal having a fractal dimension of 1.65. A small amount of residual solvent still remains in the film after spin-casting due to the high boiling temperature of DMF. This induces the lateral strain within the films during the annealing process, which further triggers the formation of the intriguing surface patterns. Autophobic dewetting is also believed to play an important role in the growth of the pattern.

Introduction

Block copolymers have been of considerable interest since they can form ordered domains in the order of the radius of gyration due to the constraint of chemical junction points between the two polymer blocks limited to the interface.[1] The microdomain structure varies depending on the composition of the block segments, and symmetric block copolymers are known to form lamellar microdomains.[1] When symmetric block copolymers are spun-cast into thin films and annealed above their glass transition temperature, the lamellae preferentially align parallel to the substrate with *symmetric* or *asymmetric* wetting depending on the interplay between the substrate interaction and the surface tension of each block.[2−4] This further causes the formation of island or hole structures with their heights quantized in $(n + {}^1/_2)$-L_0 for the asymmetric wetting or in nL_0 for the symmetric wetting since the block copolymer lamellae tend to maintain their equilibrium lamellar period L_0.[1,4−9] Up until now, only islands or holes have been observed in block copolymer thin films, which are thermodynamically stable structures. In our previous paper,[10] however, we first reported the dual morphology of islands and fractal holes in a lamellar-forming polystyrene-*block*-poly(2-vinylpyridine) (PS−P2VP) copolymer thin film having an initial thickness of $t_0 = 1.8L_0$, which is believed to be the kinetically trapped metastable structure induced by a high-boiling residual solvent. We also verified from the fractal dimension analysis that the fractal hole growth in our system follows the model for the two-dimensional cluster aggregation.[11,12]

In the present work, we further investigate various hierarchical surface topographies in block copolymer thin films depending on the initial film thickness. To this end, PS−P2VP thin films with different thicknesses were prepared by spin-coating polymer solutions in *N*,*N*-dimethylformamide (DMF)[13] onto Si substrates with native oxides on top. The resultant film contains a small amount of residual solvent due to the high boiling point of DMF ($T_b = 153$ °C). Optical (OM) and atomic force microscopies (AFM) were employed to investigate the complex thin film morphologies of block copolymers originating from the competition between lamellar ordering and slow evaporation of the residual solvent during the annealing process.

Experimental Section

Materials. A PS−P2VP copolymer having a PS weight fraction of 0.37, which was determined by H NMR, was synthesized by sequential anionic polymerization in tetrahydrofuran (THF) at −78 °C using *sec*-butyllithium as an initiator. The weight-average molecular weight, M_w, and the polydispersity index, M_w/M_n, were determined to be 111 kg/g mol and 1.16, respectively, by GPC using PS standards. Small-angle X-ray scattering (SAXS) measurements carried out at the 4C1 beamline in Pohang Light Source (PLS), Korea, revealed that our PS−P2VP forms lamellar microdomains in bulk over a wide range of temperature covered in this work. Equilibrium bulk lamellar period of the block copolymer was measured to be 50 nm at 180 °C from the relationship of $L_0 = 2\pi/q_{max}$, where q_{max} is the wavenumber at the first-order peak.

Thin Film Preparation. A Si wafer was first treated with piranha solution for 2 h and washed with deioninzed water. A 4−6 wt % solution of PS−P2VP in DMF was then spun-cast at 1000−2500 rpm onto the Si wafer with a native oxide layer. Relatively low spinning speed was used here in order to obtain films containing an appreciable amount of residual solvent. Initial film thickness was measured using a Gaertner ellipsometer with a He−Ne laser having $\lambda = 632.8$ nm.

The specimens were annealed in a vacuum oven at 180 °C, which is well above the glass transition temperatures T_g's of both blocks, for a given period of time, and then quenched to room temperature for observations with OM and AFM.

† Current address: Research Park, LG Chem, Ltd., 104-1 Moonji-dong, Yuseong-gu, Daejeon 305-380, Korea.

* To whom correspondence should be addressed. E-mail: khchar@plaza.snu.ac.kr.

10.1021/ma025793j CCC: $25.00
Published on Web 05/30/2003

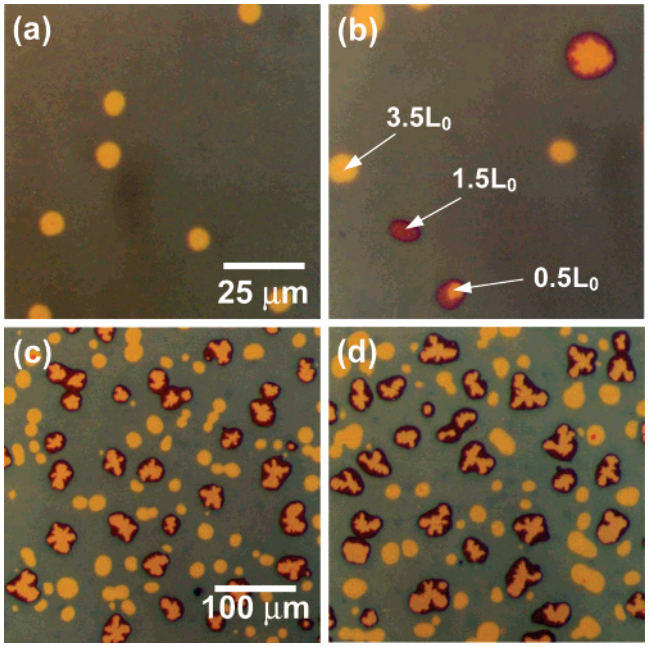

Figure 1. Optical micrographs in reflection mode for a PS−P2VP thin film with $t_0 \sim 2.5L_0$ after annealing at 180 °C in a vacuum for (a) 12, (b) 36, (c) 65.5, and (d) 89.5 h.

Optical and Atomic Force Microscopies. OM was carried out using a Nikon OPTIPHOT-2POL in reflection mode. AFM measurements were performed using a Digital Instruments Nanoscope IIIa in contact mode with a Si_3N_4 tip.

Results

As-cast specimens were observed to be featureless in reflection mode OM since they were kinetically trapped in disordered state or in ordered state with ordered grains randomly distributed along the thickness due to the spin-casting process. Annealing above the glass transition temperature of each block component, however, causes the block copolymers to order. In our system, lamellae form parallel to the substrate satisfying the asymmetric wetting condition since PS wets the surface due to its lower surface energy while P2VP preferentially saturates the silicon substrate with a native oxide due to its higher affinity.[5] This further causes the formation of islands or holes if the initial film thickness does not match the half-integer multiples of the equilibrium lamellar spacing, L_0.

Figure 1 shows optical micrographs in reflection mode for a PS−P2VP thin film with $t_0 = 125$ nm ($\sim 2.5L_0$) after annealing at 180 °C in a vacuum for different times. Typical images having various smooth regions with different heights can be clearly identified by different interference colors.[14] The circular regions with light yellow color in Figure 1a correspond to islands, as will be confirmed by the AFM measurement later. In fact, a featureless OM image is expected for the thickness ratio of $t_0/L_0 = 2.5$. The difference comes from the fact that the film thickness t_0 was measured at room temperature, while the equilibrium lamellar spacing L_0 was measured at the annealing temperature of 180 °C. If we take into account the thermal expansion of the block copolymer,[15] the film thickness at 180 °C would be slightly larger than 125 nm, and island morphology is expected in our asymmetric wetting situation to maintain the quantized thickness. The formation of islands at the initial stage of annealing has commonly been observed in block copolymer thin films.[4−9]

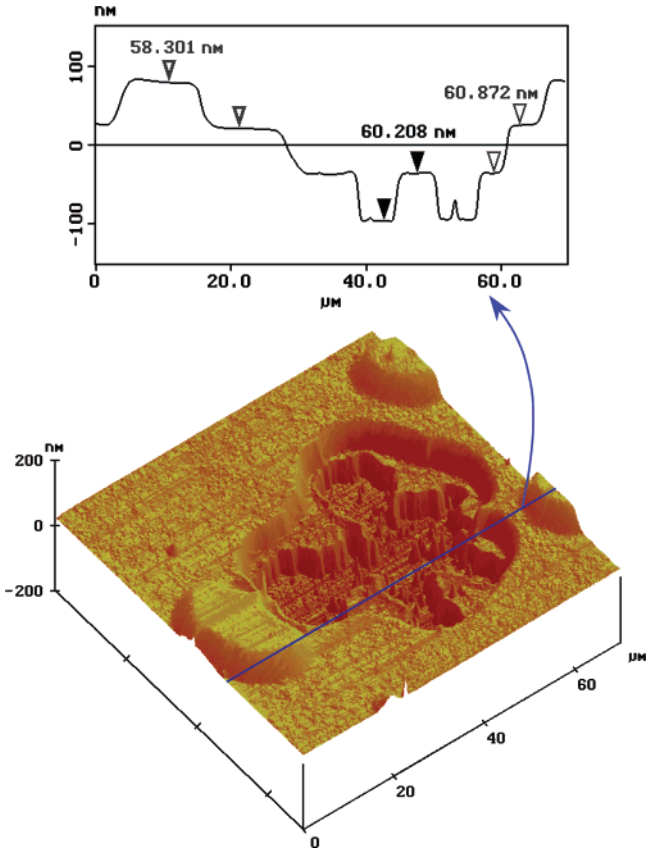

Figure 2. An AFM height image and a cross-sectional height profile of a PS−P2VP thin film with $t_0 \sim 2.5L_0$ after annealing at 180 °C for 89.5 h in a vacuum.

Further annealing, however, leads to the abnormal formation of dark brown regions and light brown fractal-like spots within the dark brown region as shown in Figure 1b. These spots correspond to holes and *fractal holes-in-holes*, respectively, as will also be confirmed by the AFM measurement below. These grow in size with annealing time as shown in Figure 1c,d. The typical size of fully grown fractal holes exceeds 40 μm, which is quite large. On the other hand, islands were also found to grow in size since the growth of the fractal holes-in-holes pushes the islands to merge. The process of the island merging is easily observed in Figure 1c,d.

AFM measurement was carried out in order to obtain accurate information on the height profile of the film. Figure 2 shows an AFM height image and a cross-sectional height profile near a *fractal hole-in-hole* in a PS−P2VP thin film with $t_0 = 2.5L_0$ after annealing at 180 °C for 89.5 h in a vacuum. Hierarchical surface topography with four flat regions of different heights is clearly shown in the image, indicating that the fractal region corresponds to the hole-in-hole with the lowest height. The cross-sectional height profile in the upper part of Figure 2 shows that both the step height of islands and the step depth of holes and hole-in-holes are about 60 nm. This value is larger than the bulk lamellar period of $L_0 = 50$ nm at 180 °C obtained from the SAXS measurements and also slightly larger than the value of 55 nm obtained from the tapping mode AFM measurements in our previous paper.[10] One possible reason for the discrepancy between the SAXS and the previous tapping mode AFM is that the interaction between PS and P2VP segments becomes more repulsive in thin films due to the effects of the substrate and the surface, enabling block copolymers to be more

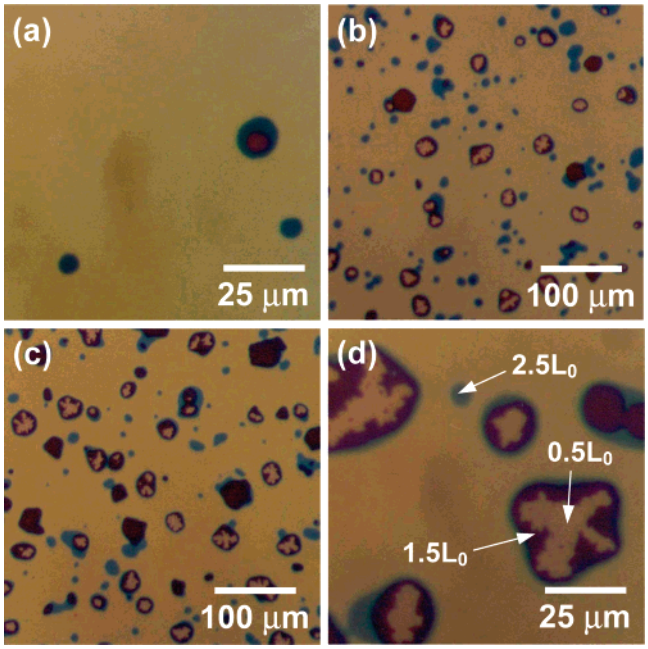

Figure 3. Optical micrographs in reflection mode for a PS−P2VP thin film with $t_0 \sim 3.3L_0$ after annealing at 180 °C in a vacuum for (a) 12 h, (b) 36 h, (c) 65.5 h with lower magnification, and (d) 65.5 h with higher magnification.

stretched perpendicular to the interface.[17] The difference between the two AFM measurements is due to the difference in AFM measurement modes. Calibration profile in tapping mode in the previous work may not be the same as the one in contact mode in the present work. It should be noted here that the bottom of the fractal hole-in-hole region is not the bare Si substrate. We found, on the basis of the AFM image of the scratched surface near a fractal hole, that the hole-in-hole has a height of 24 nm comparable to $0.5L_0$ (not shown here). This implies that the islands, holes, and fractal holes-in-holes are respectively 3.5, 1.5, and 0.5 bilayers high with respect to the substrate. This is in complete agreement with the asymmetric wetting behavior as mentioned above.

Figure 3 shows optical micrographs in reflection mode for a PS−P2VP thin film with $t_0 = 163$ nm ($\sim 3.3L_0$) after annealing at 180 °C in a vacuum for (a) 12, (b) 36, (c) 65.5 (lower magnification), and (d) 65.5 h (higher magnification). Holes are expected as the equilibrium topography for this thickness ratio. Indeed, holes with dark green color are observed at the initial stage of annealing as shown in Figure 3a. Interestingly, another hole with brown color starts to grow inside the dark green hole at 12 h. Although we observe this *hole-in-hole* morphology in Figure 3a, the number density of the *hole-in-hole* is quite small at this annealing time, as confirmed by a lower magnification OM image not shown here. As time lapses, however, the number and size of the hole-in-hole increase, and simultaneously fractal holes with light brown color are formed inside the holes-in-holes as shown in Figure 3b,c. The hierarchical surface topography is more clearly seen with four regions in different interference color in Figure 3d, which is a higher magnification version of Figure 3c.

AFM was also performed on this sample at the annealing time of 89.5 h, and the results are shown in Figure 4. Stepwise shapes inferred from the interference colors in the OM image are confirmed from the AFM height image and the cross-sectional AFM profile. Each

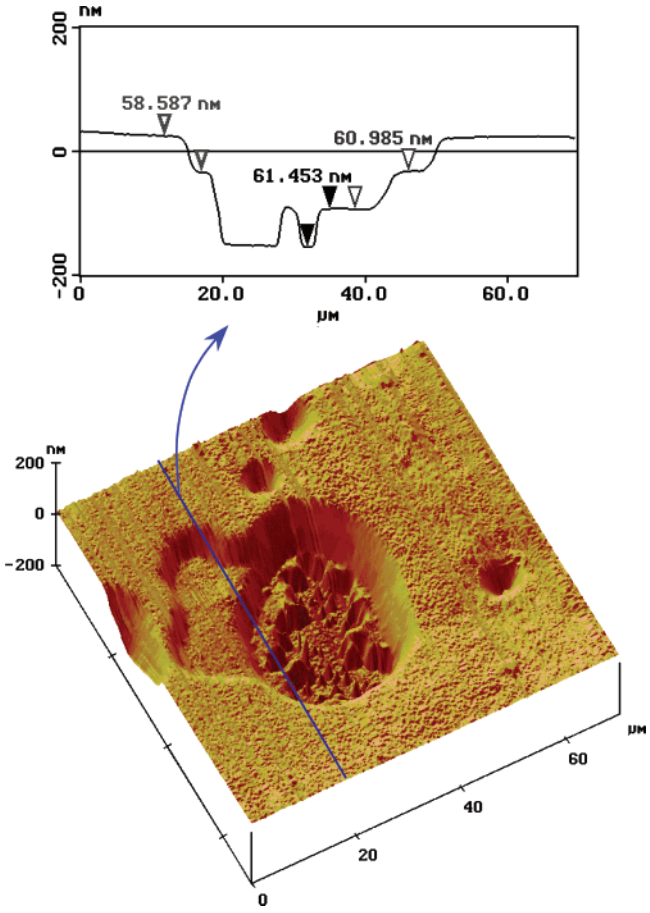

Figure 4. An AFM height image and a cross-sectional height profile of a PS−P2VP thin film with $t_0 \sim 3.3L_0$ after annealing at 180 °C for 89.5 h in a vacuum.

step height difference was again found to be about 60 nm, in agreement with the equilibrium lamellar spacing obtained from the SAXS within experimental uncertainty.

A film with a thickness smaller than $2.5L_0$ was also investigated. Figure 5 shows optical micrographs in reflection mode for a PS−P2VP thin film with $t_0 = 110$ nm ($\sim 2.2L_0$) after annealing at 180 °C in a vacuum for (a) 6, (b) 17, (c) 31, and (d) 50 h. As expected, holes with dark brown color (in 1.5 bilayer height) are formed in dark green background (in 2.5 bilayer height) at the initial stage of annealing. Further annealing again leads to the formation of light brown fractal holes (in 0.5 bilayer height) within the holes as shown in Figure 5b. These fractal holes form within nearly every hole and grow in size with annealing time as shown in Figure 5c,d. This fractal hole-in-hole growth causes the deformation of originally circular shape of dark brown holes to irregular shape. The deformation of the holes surrounding the fractal holes is also observed for the films with $t_0 = 2.5L_0$ and $3.3L_0$ (see Figures 1d and 3d). This implies that the fractal hole growth is not restricted by the surrounding holes and that it dominates the overall growth of our hierarchical surface patterns. We believe that it is related to the autophobic dewetting between the bottom brush layer and the layer adjacent to it, and this will be discussed in detail later. It is interesting to note here that the islands with light yellow color (in 3.5 bilayer height) start to form at the top layer at 50 h. This is due to the lateral pressure caused by the growth of the fractal holes-in-holes and will be elaborated in detail below.

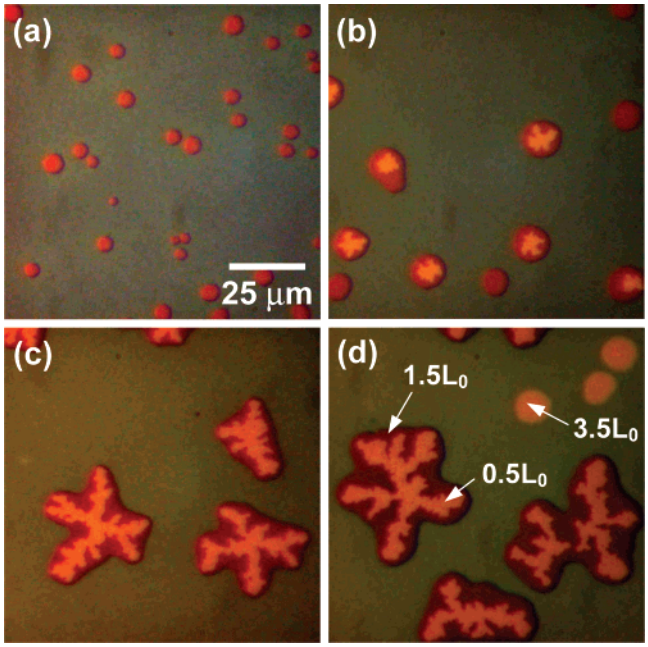

Figure 5. Optical micrographs in reflection mode for a PS−P2VP thin film with $t_0 \sim 2.2L_0$ after annealing at 180 °C in a vacuum for (a) 6, (b) 17, (c) 31, and (d) 50 h.

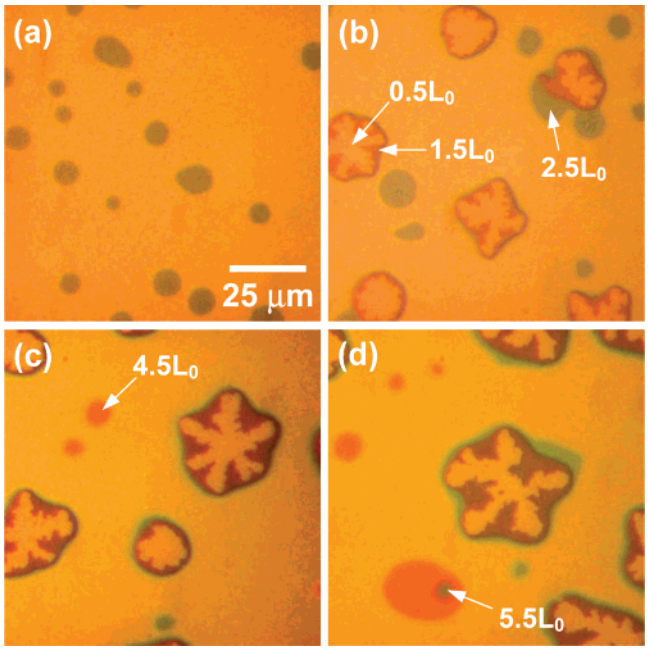

Figure 6. Optical micrographs in reflection mode for a PS−P2VP thin film with $t_0 \sim 3.1L_0$ after annealing at 180 °C in a vacuum for (a) 17, (b) 31, (c) 50, and (d) 70 h.

A film with $t_0 = 157$ nm ($\sim 3.1L_0$), which is slightly smaller than $3.3L_0$, was also investigated by OM, and the results are shown in Figure 6. Up to intermediate annealing time, overall behavior is quite similar to that of a film with $t_0 = 3.3L_0$ shown in Figure 3. Holes are observed at 17 h (Figure 6a). Stepwise hierarchical holes are observed at 31 h, and the hole shape becomes irregular due to the growth of the fractal holes adjacent to the bottom layer (Figure 6b). At longer annealing time, however, islands with orange color (in 4.5 bilayer height) start to form at the top layer at 50 h (Figure 6c) due to the lateral pressure exerted by the growth of bottom fractal holes, and they also grow in size and number with annealing time (Figure 6d). This behavior at longer annealing time is consistent with that of a film with $t_0 = 2.2L_0$. In some cases, additional islands with blue color (in 5.5 bilayer height) forms on the top of the islands as indicated by an arrow in Figure 6d (*island-on-island* structure). The detailed description for this abnormal behavior will be given in the Discussion section.

Discussion

Mechanism of Hierarchical Surface Topography Formation. The hierarchical surface topography observed in the present work is quite similar to the dual morphology of islands and fractal holes observed for a film with $t_0 = 1.8L_0$ in our previous work.[10] At short annealing time, typical island, hole, or labyrinthine structure forms depending on the initial film thickness. At long annealing time, however, the hierarchical structure consistently forms in our systems, and the fractal holes are observed only adjacent to the bottom half-lamellar brush layer.

In our previous paper, we have shown on the basis of the ellipsometry of the films before and after preannealing below T_g that the as-cast film contains about 2 wt % of residual solvent. Recent X-ray reflectivity measurements of the films before and after the preannealing supported this thickness reduction. It was also found that the fractal hole formation is significantly retarded in the partly preannealed specimens. This implies that the residual solvent affects the formation of hierarchical surface topography in our system. We propose the following mechanism as shown in Figure 7 based on these experimental evidences. The schematic is modified from the one that we proposed in the previous paper[10] in order to take into account the edge profiles of islands and holes.[18,19]

An as-cast film contains a small amount of DMF solvent (typically below 5%) due to its high boiling point (153 °C) and low spinning speed during the spin-casting. When we anneal the thin film with $t_0 \sim 2.2L_0$ at 180 °C, parallel lamellae with holes quickly develop in the presence of residual solvent due to high mobility of both PS and P2VP segments since the annealing temperature is much higher than the T_g's of both segments (Figure 7a). As shown in the figure, there exist edge dislocations on the rim of holes since the PS block has preferential affinity toward the surface on side walls as well as at the bottom of the holes. Although real edge profiles of holes or islands in the lamellar thin films have been reported to be more complicated than these, frequently showing multiple perpendicularly oriented layers near the rim,[19−22] we can simply assume the single edge dislocation at the rim for the sake of explanation. It is assumed in our schematic that only P2VP forms edge dislocation cores based on the work of Rafailovich and co-workers.[19] They observed in their lamellar PS−P2VP block copolymer thin films that P2VP always forms dislocation cores in the islands although PS and P2VP blocks are expected to have nearly the same viscosity due to the same molecular weights. The assumption is reasonable since P2VP block in our system has larger molecular weight than PS. Further annealing causes the residual solvent to evaporate completely (Figure 7b). This induces a slight reduction in the total layer thickness, thus making the lamellae strained laterally ($L_0' < L_0$) similar to the case of Korneripalli et al.[12] Lateral strain imposed on each bilayer can be removed by adjusting its step height L_0' to the equilibrium domain period L_0. This involves the lateral area reduc-

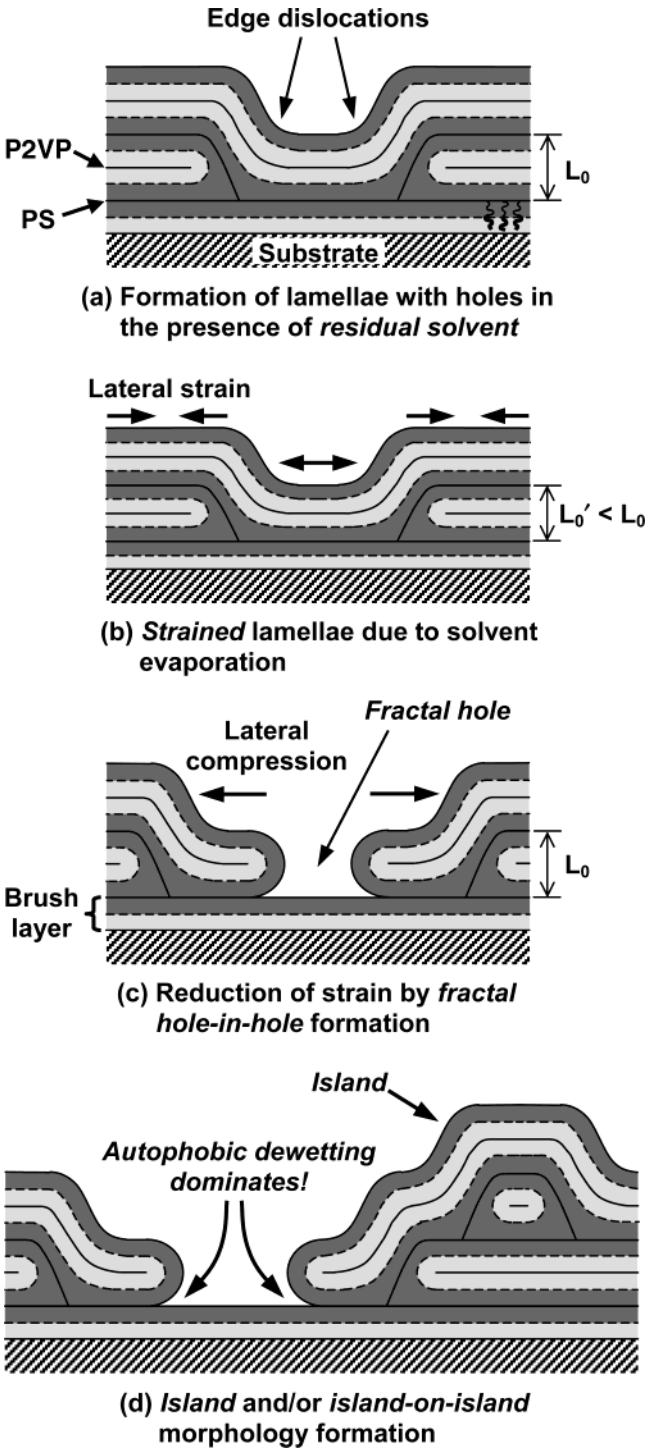

Figure 7. Schematic of hierarchical surface topography formation with annealing in our block copolymer thin film with $t_0 \sim 2.2L_0$ induced by residual solvent and autophobic dewetting. The dark and gray regions correspond to PS and P2VP, respectively. The dotted lines represent the PS/P2VP interface while the solid lines represent PS/PS or P2VP/P2VP separations originating from two different block chains.

tion of each layer in order to keep the segmental density constant. In the case of the top bilayer, this is achieved by expanding the lateral dimension of the holes through the lateral diffusion of block copolymer chains through edge dislocations connecting the top bilayer to the holes as shown in the figure. On the other hand, the strained bilayers below the top bilayer cannot easily attain their equilibrium domain period without a rupture of the layer (Figure 7c). This leads to the formation of *hole-in-hole* structure as shown in Figure 5b−d. Although the schematic shown in Figure 7 is for the film with $2.0L_0 < t_0 < 2.5L_0$, the same mechanism is applied to other films with different thicknesses. For thicker films with a total number of bilayers higher than 2.5, the rupture of the layers occurs *hierarchically* in series from the top to the bottom layer as shown in Figures 1, 3, and 6 for the films with $t_0 = 2.5L_0$, $3.3L_0$, and $3.1L_0$, respectively.

One possible way to achieve L_0 while maintaining the original hole or island structure is the diffusion of block copolymer chains in a direction normal to the lamellar layer. However, this cross diffusion is highly restricted compared with the lateral diffusion parallel to the lamellar layer since the block copolymer chains should pass through the strongly segregated region in the former case.[23]

We do not consider in the above schematic the possible domain spacing difference originating from the residual solvent in the film. If we assume that DMF used in our study is a nonselective solvent for PS and P2VP, the residual solvent decreases the effective interaction parameter χ_{eff} between the PS and the P2VP blocks according to the screening effect. χ_{eff} has been well approximated as the product of polymer volume fraction and interaction parameter.[24] If we assume that the film approximately contains 2% of the residual solvent and use the scaling relationship of $L_0 \sim \chi^{1/6}$ in the strong segregation limit,[1] it is estimated that there is about 0.3% increase of the lamellar domain spacing after the removal of solvent. This is negligible compared with 2% reduction of L_0 due to the thickness reduction after solvent removal.

Fractal Hole Formation near Bottom Brush Layer. PS−P2VP is well-known to form a brush layer with half of a lamellar period adjacent to the substrate due to the strong interaction of P2VP block to the substrate in a thin film. As we have shown in the OM images of Figures 1, 3, 5, and 6, the hole growth near the bottom brush layer after the rupture consistently follows the *fractal growth*. This is quite intriguing since the hole growth in layers other than the one adjacent to the bottom brush layer shows typical circular shape. This can also be explained by the schematic shown in Figure 7c. Since the block copolymer chains in bottom brush layer are tightly attached to the substrate, the brush layer is quite stable. Therefore, the edge profiles of the holes adjacent to the brush should have $s = +1/2$ disclinations, which are completely different from the edge dislocations observed in the holes in the above bilayers, as shown in Figure 7c. The PS blocks in the second bilayer *autophobically* dewet the PS blocks in the bottom brush layer. This is believed to induce the fractal patterns observed in our system and will be discussed later.

Quantitative analysis of the edge angles can give indirect evidence on the edge profiles assumed in the schematic of Figure 7. The edge angles of terraces in each bilayer were calculated from the AFM height images shown in Figures 2 and 4, and the results are summarized in Table 1. It should be mentioned here that the edge angle is defined as the angle of the slope at the half-height of the terrace and that each value in Table 1 is the average of at least 20 cross-sectional height profiles. As shown in Table 1, the edge angles of islands, holes, and holes-in-holes are nearly the same within experimental uncertainty although the edge

Table 1. Edge Angles (deg) Obtained from the AFM Data Shown in Figures 2 and 4

initial film thickness	island	hole	hole-in-hole	fractal hole-in-hole or fractal hole-in-hole-in-hole
$t_0 = 2.5L_0$	2.0 ± 0.52	2.5 ± 0.46		5.5 ± 1.1
$t_0 = 3.3L_0$		2.5 ± 0.43	2.8 ± 0.53	5.0 ± 0.79

angle of islands is slightly smaller than that of holes or holes-in-holes. On the other hand, the edge angles of fractal holes are as twice as those of holes, holes-in-holes, or islands. This is in good agreement with the schematic shown in Figure 7c,d. Although the real edge profiles of fractal holes should be smoothed out due to the chain stretching or the formation of perpendicularly ordered structures at the rims as noted by Rafailovich and co-workers,[19] their edge angles are expected to be larger than those of the simple islands or holes which have edge dislocation structures.

Fractals in our system are quite similar in shape to nonequilibrium patterns[12,25−30] observed in other systems such as metal dendrites grown by electrodeposition,[28] two-dimensional crystallites grown on a rough surface,[29] viscous fingering patterns in a radial Hele−Shaw cell,[30] and the hole growth in a strained block copolymer lamellae.[12] Particularly, the result reported by Koneripalli et al.[12] is quite informative to our study. They prepared a $^3/_2$ bilayer film of a symmetric PS−P2VP diblock copolymer compressed to a thickness of $1.45L_0$ by a confinement technique followed by annealing. Subsequent annealing after the removal of the confinement layer led to the development of fractal holes quite similar in form to ours. They attributed the fractal hole formation, which is governed by the Laplace equation with moving boundary conditions, to the heterogeneous nucleation by tiny dust particles in laterally strained lamellae. In the previous paper,[10] we have shown from the fractal dimension analysis that the fractal hole observed in our film with $t_0 = 1.8L_0$ has a fractal dimension d_f of 1.65, in exact agreement with $d_f = {}^5/_3$ from the mean-field theory for *two-dimensional diffusion-controlled cluster formation* proposed by Muthukumar.[11] We also performed the fractal dimension analysis (not shown here) for a fully developed fractal hole-in-hole structure shown in Figure 5d. Although it is surrounded by the hole with dark brown color, it shows nearly the same fractal dimension, implying that the fractal hole growth adjacent the brush layer is not restricted by the surrounding holes. This point will be elaborated below.

Evolution of Hierarchical Surface Morphology with Prolonged Annealing: Autophobic Dewetting. Although the lateral stress induced by the residual solvent is believed to trigger the formation of hierarchical holes in our systems, the additional island and/or *island-on-island* morphology at long annealing time shown in Figures 5d and 6c,d cannot be explained by the strain release mechanism alone. It needs more detailed analysis.

To this end, low-magnification OM was carried out for the films with $t_0 = 2.2L_0$ and $3.1L_0$ at prolonged annealing time, and the resulting images are shown in Figures 8 and 9, respectively. Image analysis was then performed for these films in order to obtain quantitative information on the growth process of hierarchical surface patterns. Figures 10 and 11 show the time evolution of the fractional coverage and the number density of each hierarchical region during annealing at 180 °C for the films with $t_0 = 2.2L_0$ and $3.1L_0$, respectively. It should be noted here that the analysis was performed over the area of at least 8.75×10^5 μm^2, which is 5.2 times larger than the total image area shown in Figures

Figure 8. Lower magnification optical micrographs in reflection mode for a PS−P2VP thin film with $t_0 \sim 2.2L_0$ after annealing at 180 °C in a vacuum for (a) 31, (b) 50, (c) 70, and (d) 98 h.

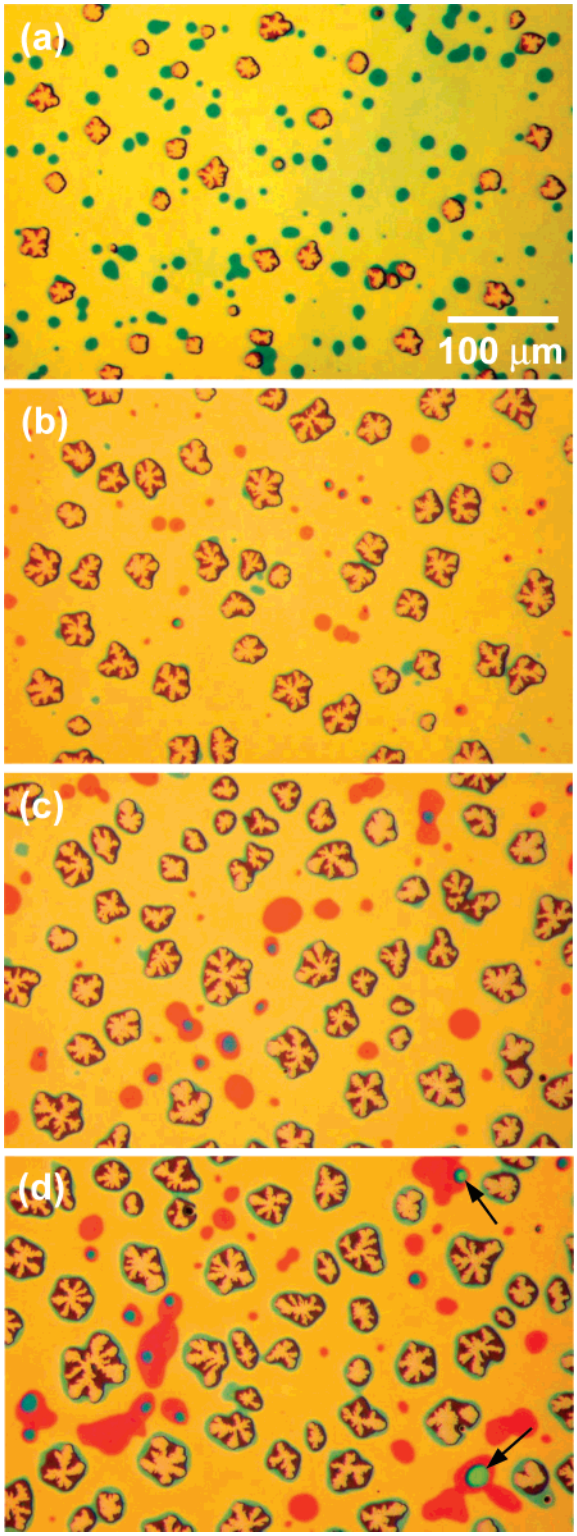

Figure 9. Lower magnification optical micrographs in reflection mode for a PS−P2VP thin film with $t_0 \sim 3.1L_0$ after annealing at 180 °C in a vacuum for (a) 31, (b) 50, (c) 70, and (d) 98 h.

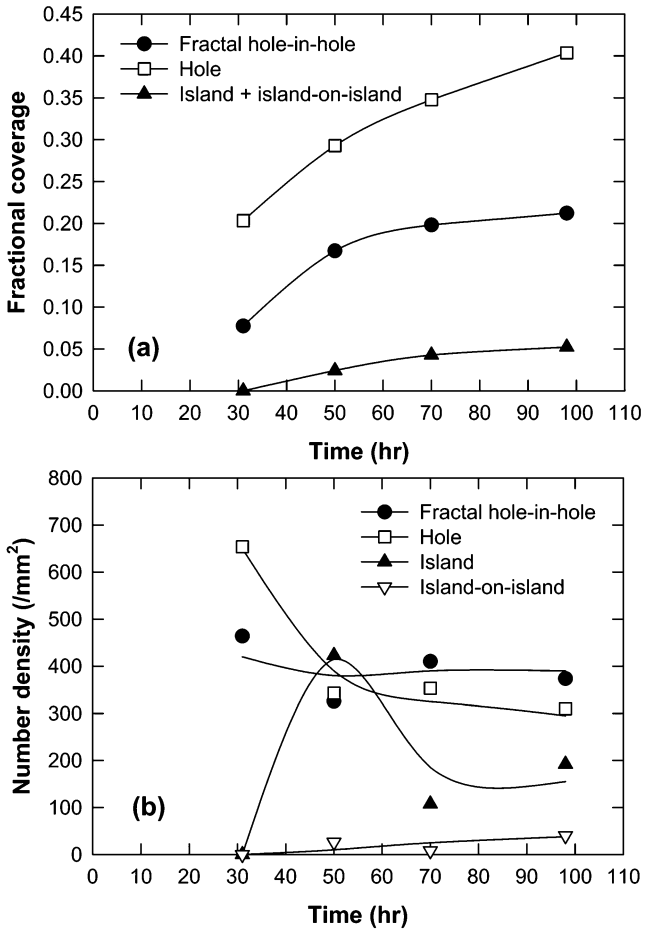

Figure 10. Evolution of (a) fractional coverage and (b) number density of holes, islands, and fractal hole-in-holes for a PS−P2VP thin film with $t_0 \sim 2.2L_0$ during annealing at 180 °C. All data are obtained from the image analysis over the area of 8.75×10^5 μm^2, which is 5.2 times larger than the OM images shown in Figure 8.

8 and 9, to achieve good statistics. In Figures 8a and 9a, fractal holes have already formed inside the holes at 31 h. The number of hierarchical fractal holes is 464 and 235/mm^2 at this time as can be seen in Figures 10b and 11b. However, many small holes still exist without further hierarchical structure within them as can be seen in Figures 8a and 9a. These amount to about 29% of total number of holes for the film with $t_0 = 2.2L_0$ and 75% for the film with $t_0 = 3.1L_0$ as shown in Figures 10b and 11b, respectively. It is quite interesting to note that these holes nearly vanish at 50 h as the hierarchical holes grow in size due to the growth of the fractal holes within them. Almost every hole in Figures 8b and 9b contains the hierarchical fractal hole. It is clear from Figures 10b and 11b that the total number of holes dramatically decreases at 50 h and reaches a plateau value, which is nearly the same as the number of hierarchical fractal holes, while the number of fractal holes is nearly constant with annealing time. This implies that the number of holes without hierarchical structure decreases not because hierarchical structures form within them but because they are filled up by the lateral compression force exerted during the growth of other hierarchical holes.

We mentioned that the fractal hole growth near the bottom brush layer of $L_0/2$ thickness occurs through the *autophobic dewetting*. It has commonly been observed in block copolymer thin films slightly above the order−disorder transition temperature that fairly large disordered droplets autophobically dewet the substrate-induced dense *brush* layer of ordered copolymer chains.[17,31] It is also reported that polystyrene homopolymer dewets polystyrene brush layer attached to the substrate under certain conditions.[32] Autophobic dewetting in our system, however, is different since it occurs below the order−disorder transition temperature

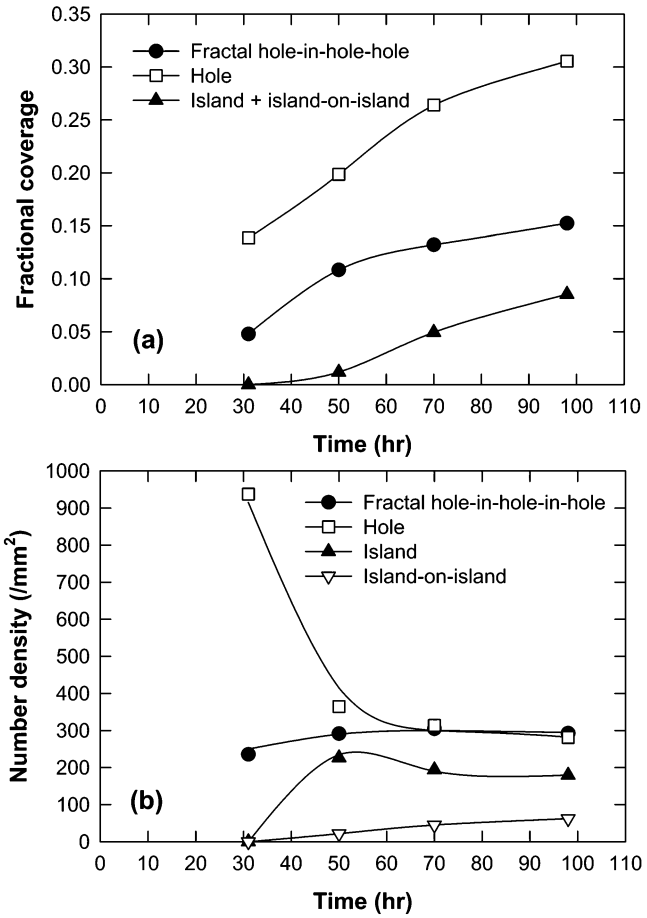

Figure 11. Evolution of (a) fractional coverage and (b) number density of holes, islands, and fractal hole-in-hole-in-holes for a PS−P2VP thin film with $t_0 \sim 3.1L_0$ during annealing at 180 °C. The data at 31 and 50 h are obtained from the image analysis over the area of 8.75×10^5 μm^2, which is 5.2 times larger than the OM images shown in Figure 9, and the data at 70 and 98 h are obtained over the area of 1.75×10^6 μm^2.

at a height of $0.5L_0$ between the *ordered* PS brush attached to the substrate and another *ordered* PS brush in direct contact with it as schematically shown in Figure 7c. It should be noted here that the thickness of the bottom half-lamellar brush layer tightly bound to the substrate was found to be 24 nm from the tapping mode AFM measurement of the scratched surface. Since L_0 from the tapping mode AFM is 55 nm, it is slightly smaller than $L_0/2$. This means that the chain packing in the bottom layer is slightly less than the above layer probably due to the strong attraction between P2VP chains and the native silicon oxide layer on the substrate. This packing difference together with the lateral stress mentioned above gives the origin for the autophobic dewetting in our system.

In Figures 10a and 11a, the fractional coverage of hierarchical fractal holes gradually increases with annealing time. The fractional coverages of holes and islands also increase gradually with annealing time since materials should move to the layers above in order to conserve mass during the growth of the fractal hole-in-hole (or hole-in-hole-in-hole) region. These observations are contrary to the fact that the fractional coverage of holes or islands in conventional block copolymer thin films, which have either holes or islands, is constant after initial annealing time.[6,33] It is reported that island (or hole) growth in block copolymer thin films follows the 2D Ostwald ripening mechanism by surface diffusion and that $\langle R \rangle \sim t^{1/3}$ and $N \sim t^{-2/3}$, where $\langle R \rangle$ and N are the average size and the number of islands (or holes), respectively.[33] This power law dependence was found not to be valid for the island (or hole) growth at the top layer in our system mainly because the fractional coverage in our system is not conserved during annealing due to the autophobic dewetting adjacent to the bottom brush layer. This implies that the fractal hole growth adjacent to the bottom brush layer is not restricted by the surrounding holes, therefore dominating the growth process of the hierarchical surface topography in our thin films. The dominant growth of the hierarchical fractal holes through the autophobic dewetting deforms the originally circular shape of surrounding holes into irregular shape as mentioned above and finally exerts lateral compression force on the top bilayer as illustrated in Figure 7c, causing the reduction of its area. To accomplish this, the holes without hierarchical structure should be first filled up. After filling up most of the holes, islands should form at the top layer in order to reduce the lateral force imposed on the layer, as shown in light yellow color in Figure 8b and in orange color in Figure 9b. This process is schematically illustrated in Figure 7d. As the hierarchical structure grows further with annealing, the merge between islands starts to induce the growth of islands as shown in Figures 8c and 9c, and consequently the number of islands decreases at 70 h as shown in Figures 10b and 11b. The island merging is more clearly seen at longer annealing time as shown in Figures 8d and 9d. We mentioned before that in some cases additional islands form at the top of the first island in these two films, showing the intriguing *island-on-island* morphology. This is also caused by the lateral compression force at the top layer exerted by the growth of the hierarchical hole structures. As shown in Figure 7d, the islands formed have edge defects such as edge dislocations. These defects can act as diffusion channels for the block copolymer chains. If the free energy barrier for additional island formation at the top of the first island is sufficiently low, the *island-on-island* morphology would be developed. Sometimes, *island-on-island-on-island* morphology is also observed as indicated by the arrows in Figures 8d and 9d. It is uncertain at this point which has a lower energy barrier between the formation of islands at the top layer or the formation of additional islands at the top of islands. However, this is beyond the scope of this paper and will not be discussed in detail.

We note that the hierarchical hole growth originating from the fractal hole growth is slightly faster in these films with $t_0 = 2.2L_0$ and $3.1L_0$ than in the film with $t_0 = 3.3L_0$. In addition, the fractals for the former shown in Figures 5 and 6 contain sharper branches than the fractal branches observed for the film with $t_0 = 3.3L_0$ shown in Figure 3. This is because the film thickness difference from the half-integer multiples is larger in these films. In this case, the initial hole size is supposed to be larger, providing more space for the rupture of the layer and less restricting the initial growth of the pattern. Therefore, it is easier to form the hierarchical hole in these films, and its fractal growth is faster. This also explains the development of the additional island and/or island-on-island morphology in the former films at prolonged annealing time since the faster growth of the fractals through the autophobic dewetting will exert much more compression force onto the above layers. The

film with $t_0 = 2.5L_0$ shows the island morphology initially, which is different from the other three films. In this case, the rupture of the layer can be retarded since the strain induced in the layer can first be released by the annihilation of islands through the diffusion of block chains from the island to the top layer. This is why the fractal pattern formation in this film is found to be quite slow compared with the other films initially forming holes.

Metastability of Hierarchical Surface Topography. The hierarchical surface topography observed in our system is not the thermodynamically stable structure but the *metastable* structure kinetically induced by the residual solvent. Although hole or island morphology has the lowest free energy at a given annealing temperature, it is not attained with prolonged annealing since the irreversible autophobic dewetting of the fractal holes is dominant at longer annealing time. This kinetically arrested nonequilibrium hierarchical morphology was found to be stable during prolonged annealing at 180 °C up to 5 days, indicating *metastability*.

Conclusion

We have investigated for the first time the various *hierarchical surface topographies* in block copolymer thin films with initial thicknesses of $2.0L_0 < t_0 < 3.5L_0$, which were obtained by the spin-coating process using a high boiling solvent at a relatively low spinning speed. The development of hierarchical holes is triggered by the lateral strains induced by the postevaporation of a small amount of the residual high boiling solvent after the facile development of parallel lamellae with holes or islands depending on the initial thickness. The rupture of the film occurred from top to bottom layer. The hole structure adjacent to the bottom brush layer was found to be always fractal contrary to the typical circular holes. This is believed to be related to the *autophobic dewetting* between the brush layer tightly bound to the substrate and the layer above it. This *autophobic dewetting* dominates the pattern growth process of our system at longer annealing time, and it further exerts compression force onto the layers above. This eventually causes the development of another intriguing hierarchical morphology such as island, *island-on-island*, and *island-on-island-on-island* morphologies. Thin films with hierarchical patterns created in present work are believed to be a promising candidate for nonglossy coating materials since it can virtually deflect the incident light in random direction due to their various edge profiles present.

In present paper, we only investigated the effect of initial film thickness on the hierarchical topography. In addition to the initial film thickness, the composition asymmetry of the block copolymer and the brush density in the $L_0/2$ layer adjacent to the substrate can also affect the hierarchical morphology growth in our system. The detailed discussion of these effects, however, is beyond the scope of present paper and will be addressed in a future publication.

Acknowledgment. This work was funded in part by the National Research Laboratory program (Grant M1-0104-00-0191). Financial support from the Korean Ministry of Education through the Brain Korea 21 Program and from the Korean Ministry of Science and Technology (MOST) under Grant 99-07 is also greatly acknowledged. SAXS experiments performed at PLS were supported in part by MOST and POSCO. We thank Dr. S.-H. Chu for helping us with the ellipsometric measurement of film thickness.

References and Notes

(1) Hamley, I. W. *The Physics of Block Copolymers*; Oxford University Press: New York, 1998.
(2) Russell, T. P.; Coulon, G.; Deline, V. R.; Miller, D. C. *Macromolecules* **1989**, *22*, 4600.
(3) Menelle, A.; Russell, T. P.; Anastasiadis, S. H.; Satija, S. K.; Majkrzak, C. F. *Phys. Rev. Lett.* **1992**, *68*, 67.
(4) Mansky, P.; Russell, T. P.; Hawker, C. J.; Pitsikalis, M.; Mays, J. *Macromolecules* **1997**, *30*, 6810.
(5) Coulon, G.; Ausserre, D.; Russell, T. P. *J. Phys. (Paris)* **1990**, *51*, 777.
(6) Coulon, G.; Collin, B.; Ausserre, D.; Chatenay, D.; Russell, T. P. *J. Phys. (Paris)* **1990**, *51*, 2801.
(7) Krausch, G. *Mater. Sci. Eng.* **1995**, *R14*, 1.
(8) Heier, J.; Kramer, E. J.; Groenewold, J.; Fredrickson, G. H. *Macromolecules* **2000**, *33*, 6060.
(9) Smith, A. P.; Douglas, J. F.; Meredith, J. C.; Amis, E. J.; Karim, A. *Phys. Rev. Lett.* **2001**, *87*, 15503.
(10) Lee, S.-H.; Kang, H.; Cho, J.; Kim, Y. S.; Char, K. *Macromolecules* **2001**, *34*, 8405.
(11) Muthukumar, M. *Phys. Rev. Lett.* **1983**, *50*, 839.
(12) Koneripalli, N.; Bates, F. S.; Fredrickson, G. H. *Phys. Rev. Lett.* **1998**, *81*, 1861.
(13) DMF is known as a universal solvent and dissolves both PS and P2VP well although it is slightly selective toward P2VP.
(14) The colors shown in Figure 1 are not the calibrated ones and do not exactly match the Newton's interference colors expected from the thicknesses indicated. We think that the main difference comes from the fact that the observed color slightly varies depending on the intensity of light going into the camera.
(15) The film thickness at 180 °C would be 131 nm, and t_0/L_0 is now 2.6 if we use 1.030 and 0.9817 g/cm^3 for the density of PS at 100 and 180 °C, respectively, in ref 16 and assume that PVP has the same thermal expansion coefficient as PS. Here, we used a value at 100 °C, which is the glass transition temperature of PS, instead of a value at 25 °C, since the film was vitrified during the spin-casting process.
(16) Brandrup, J.; Immergut, E. H. *Polymer Handbook*, 3rd ed.; Wiley-Interscience: New York, 1989; p V/82.
(17) Limary, R.; Green, P. F. *Macromolecules* **1999**, *32*, 8167.
(18) Maaloum, M.; Ausserre, D.; Chatenay, D.; Coulon, G.; Gallot, Y. *Phys. Rev. Lett.* **1992**, *68*, 1575.
(19) Liu, Y.; Rafailovich, M. H.; Sokolov, J.; Schwarz, S. A.; Bahal, S. *Macromolecules* **1996**, *29*, 899.
(20) Heier, J.; Kramer, E. J.; Walheim, S.; Krausch, G. *Macromolecules* **1997**, *30*, 6610.
(21) Carvalho, B. L.; Thomas, E. L. *Phys. Rev. Lett.* **1994**, *73*, 3321.
(22) Peters, R. D.; Yang, X. M.; Nealey, P. F. *Macromolecules* **2002**, *35*, 1822.
(23) Hamersky, M. W.; Tirrell, M.; Lodge, T. P. *Langmuir* **1998**, *14*, 6974.
(24) Sakurai, S.; Hashimoto, T.; Fetters, L. J. *Macromolecules* **1996**, *29*, 740.
(25) Vicsek, T. *Fractal Growth Phenomena*; World Scientific: Teaneck, NJ, 1989.
(26) Takayasu, H. *Fractals in the Physical Sciences*; Manchester University Press: New York, 1990.
(27) Meakin, P. *Fractals, Scaling and Growth far from Equilibrium*; Cambridge University Press: New York, 1998.
(28) Matsushita, M.; Sano, M.; Hayakawa, Y.; Honjo, H.; Sawada, Y. *Phys. Rev. Lett.* **1984**, *53*, 286.
(29) Ben-Jacob, E.; Deutscher, G.; Garik, P.; Goldenfeld, N.; Lereah, Y. *Phys. Rev. Lett.* **1986**, *57*, 1903.
(30) Daccord, G.; Nittmann, J.; Stanley, H. E. *Phys. Rev. Lett.* **1986**, *56*, 336.
(31) Hamley, I. W.; Hiscutt, E. L.; Yang, Y.-W.; Booth, C. *J. Colloid Interface Sci.* **1999**, *209*, 255.
(32) Maas, J. H.; Cohen Stuart, M. A.; Leermakers, F. A. M.; Besseling, N. A. M. *Langmuir* **2000**, *16*, 3478.
(33) (a) Bassereau, P.; Brodbreck, D.; Russell, T. P.; Brown, H. R.; Shull, K. R. *Phys. Rev. Lett.* **1993**, *71*, 1716. (b) Ardell, A. J. *Phys. Rev. Lett.* **1995**, *74*, 4960. (c) Bassereau, P.; Brodbreck, D.; Russell, T. P.; Brown, H. R.; Shull, K. R. *Phys. Rev. Lett.* **1995**, *74*, 4961.

MA025793J